Thermal Analysis of Palm Stearine by DSC

W. Ken Busfield*,[a] and **Peter N. Proschogo**[b]

[a]Division of Science and Technology, Griffith University, Nathan, Brisbane, Queensland, 4111, Australia and [b]Meadow Lea Foods, Murarrie, Brisbane.

The chemical composition and thermal properties of palm stearine have been investigated. The sample consists of triglycerides containing mainly the fatty acid residues: palmitic (P) 51.4%; oleic (O) 32.7%; linoleic (L) 8.3% and stearic (S) 5.0%. The sample melts as almost two independent components in separate temperature ranges. DSC analysis and analogy with the work of Persmark *et al.* (1) indicate that the high melting component, consisting mainly of the triglycerides POP (33%), PPP (~15%), POS (4%) and PPS (2%), crystallizes initially in an α crystal form which rearranges on tempering successively to β' and β crystal forms. The constitution of the lower melting component is much more dependent on thermal history but is mainly POO (14% overall), PLP (13% overall) and SOO (1% overall). It crystallizes initially in a sub α form which rearranges to β' when tempered at 0°C and to the β crystal form when tempered at 10°C. The liquid phase contains mainly PLO (8% overall), OOO (6% overall), PLL (4% overall) and LOO (1% overall).

Palm stearine, a high melting point fraction from palm oil, can be used in the manufacture of edible fat products. A fundamental understanding of its physical state and the factors which control the physical state, such as thermal treatment and hydrogenation, is of importance for the control of product quality and for the possible extension of the range of products. Although there have been several investigations of the physical state of unfractionated palm oil (1-6), few have dealt with palm stearine (7,8).

In common with other triglycerides, the morphology of palm stearine is strongly dependent on the thermal history of the sample. This is due to the complex crystal polymorphism exhibited by the system—a consequence of the range of packing modes available to the fatty acid residues in triglycerides. The morphology directly influences such important properties as melting point, softening point, solids content, plasticity and brittleness. It can be controlled to a certain extent by tempering (annealing) and by the rate of cooling from the molten state, and it can be modified by hydrogenation, the subject of the next paper in this series (9).

The packing modes available to triglycerides are normally labelled sub-α, α, β' and β (10). The latter is the most highly ordered and closely packed and, hence, is the most stable crystal form (11). It is the least likely structure to be formed by crystallization directly from the melt, except for the case of fats consisting of predominantly one triglyceride type. Mixed triglycerides generally crystallize from the melt in the less closely packed α or sub-α structures, where the greater variance of triglyceride composition can be accommodated. Even the pure triglyceride, tripalmitin, crystallizes in the α form when cooled quickly (12). The formation of β' or β structures requires slower cooling, tempering or solution crystallization.

*To whom correspondence should be addressed.

In this paper an investigation of the chemical constitution of a typical palm stearine sample by GC and HPLC techniques together with a study of the physical characteristics by NMR and DSC techniques is described. The DSC investigation includes the effects of tempering and heating rates on the crystalline content and its stability.

EXPERIMENTAL

Material. The palm stearine sample was typical of the material used in the production of margarines and shortenings in Australia. It was supplied by Meadow Lea Foods Ltd. It was derived from crude palm oil by a dry fractionation process in which the lower melting fraction is removed by centrifugation or filtration.

Chemical composition. Three methods were used: (i) GC of fatty acid methyl esters after transesterification: Transesterification was by a slight modification of the method described by Metcalfe and Wang (13). GC analysis was performed on a 50 m W.C.O.T. vitreous silica capillary column coated with CP-SIL 88 from Chrompak in a Varian 3700 GC instrument. Hydrogen was used as carrier gas, and optimum separation was achieved with a temperature program from 175-190°C. Peak identification and area measurement were done on a Perkin-Elmer 10 B Data Station which had been precalibrated with standard reference samples. (ii) GC triglyceride analysis: The analysis was performed on a 3.5 m W.C.O.T. fused silica capillary column coated with OV101 in a Perkin-Elmer Sigma 2B GC instrument. Hydrogen was used as carrier gas. Optimum separation conditions were achieved with a column temperature program of 100°C to 270°C at 40°C min^{-1} and then to 330°C at 10°C min^{-1}. Peak areas were obtained from a Shimadzu C-RIA Chromotopak Integrator. Triglycerides with identical carbon number (CN) cannot be resolved by this technique. (iii) HPLC triglyceride analysis: Separations were performed on an Altex-Ultrasphere O.D.S. column, 150 mm length, with THF/acetonitrile (volume ratio = 35:65) as eluent operating at room temperature. The instrument was a Perkin-Elmer Series 2 LC; peak integration was done with a Shimadzu C-RIA Chromotopak Integrator. Detection was by UV (214 nm); extinction coefficients were based on those measured for the pure triglycerides: tristearine, triolein, trielaidin and trilinolein. Peak identification was based on relative retention times reported in the literature (8,10).

Iodine values. Iodine values were measured by the standard AOCS method Cd 1-25 (14).

Shot melting point. The shot melting point is a measure of the softening point of fats used by several food manufacturers in Australia. It is based on the method described by Barnicoat (15), sometimes referred to as 'the falling ball method,' and differs from the standard AOCS method Cc 3-25 (14). Reproducibility has been tested (16) and is described as good.

In the shot melting point determination, a calibrated tube filled to a depth of 26 mm with the fat under test is held at 60°C for 20 min; at 0°C for 10 min and at 10°C for 3 hr. It is then heated at 0.3°C min^{-1} with a metal

ball, diameter 3 mm, mass 129 mg, sitting on the surface. The shot melting point is defined as the temperature at which the ball has dropped to a depth of 13 mm. Previous experience has shown that the shot melting point is about 1° above the softening point determined by the AOCS method.

Solid fat content by NMR. The instrument was a Bruker Minispec P20i 20 Mhz NMR Spectrometer. Calibration was by standards provided by Bruker. Two types of experiments were carried out: (i) An NMR tube containing 2.5 ml sample was heated at 60°C for 10 min prior to immersion at 0°C for 60 min. The solid fat content was then measured between successive tempering procedures for 30 min at 10°, 20°, 30°, 45° and 50°C. The treatment is similar to IUPAC method 2, 323 (17). (ii) Rates of solidifcation were determined at 0° and 20°C by first heating an NMR tube containing 2.5 ml sample at 60°C for 10 min, transferring the tube to a 0° or 20°C thermostat bath and measuring the solid fat content at suitable time intervals.

Thermal analysis by DSC. The instrument was a Perkin-Elmer DSC 2C. Helium was the carrier gas and calibration was with cyclohexane. Experiments were of two types: (i) Heating rate experiments: Samples were cooled from the melt (70°C) at 80° min^{-1} to 0°C, held for 6 sec at 0°C to stabilize the instrument (as indicated by the instrument control light), and then thermograms were recorded at heating rates of 10°, 20°, 40° and 80° min^{-1}. (ii) Tempering experiments: Samples were cooled from the melt at 80° min^{-1} to 0°C and held for tempering times of 0.1 to 20 min before recording the thermograms at 10° min^{-1}. For the higher tempering temperatures of 10 and 17°C the samples were tempered first at 0°C for 10 min and then heated to the tempering temperature at 10° min^{-1}, held there for 10 min before recording the thermogram. The temperature treatment for the tempering experiment at 10°C for 30 hr was carried out in thermostat baths.

RESULTS AND DISCUSSION

Chemical composition. The results of GC and HPLC analyses are given in Tables 1 and 2. None of the methods gives a unique complete analysis. There are problems of resolution with the direct triglyceride analysis by GC and by HPLC, and the fatty acid methyl ester method gives no indication of how the fatty acids are distributed among the triglycerides. The results are reasonably self-consistent, and both sets of GC data fall within the ranges given for typical palm stearine samples by Rossell *et al.* (2).

The iodine value, which denotes the level of unsaturation in the sample, is 44. The measured value is in agreement with values of 43 and 42 calculated on the basis of the fatty acid methyl ester and the HPLC analyses, respectively.

Physical properties by NMR. The solid fat content of the palm stearine sample, measured by the NMR technique, is shown as a function of temperature in Figure 1. This clearly indicates that palm stearine melts over a broad temperature range similar to many other fats, with the solids content reducing to 3.5% at 50°C. On the basis of observations made by Timms (18), this suggests that the AOCS softening point is slightly less than 50°C, which is in agreement with the measured value of the shot melting point, 50.7°C. Previous work carried out at Meadow Lea Foods has shown that the shot melting point is about one degree above the AOCS softening point.

The NMR method was also used to study the rate at which the sample of palm stearine solidifies at 0°C and at 20°C (Fig. 2). At 20°C the solidification process is relatively smooth—although it is interesting to note that even after 60 min the solids content had only reached 44%—compared with the value of 52% observed when the sample was heated in stages up to 20°C (Fig. 1). This illustrates the effect of thermal history on the solidification characteristics. At 0°C, solidification is clearly a two-stage process; the second stage becomes apparent after about 52% solidification has occurred and after 14 to 16 min have elapsed. A further 18 to 20% of the sample solidifies in this second stage.

TABLE 1

Fatty Acid Residue Composition of Palm Stearine by GC Analysis of the Fatty Acid Methyl Esters

Fatty acid	Chain length	Content	Calc. % by mass[a]	Range[b]
Lauric	C_{12}	0.2		0.1-0.2
Myristic	C_{14}	1.2		1.0-1.3
Palmitic (P)	C_{16}	51.4	55	46.5-68.9
Palmitoleic	$C_{16:1}$	0.2		0-0.2
Stearic (S)	C_{18}	5.0	3	4.4-5.5
Oleic (O)	$C_{18:1}$	32.7	32	19.9-38.4
Linoleic (L)	$C_{18:2}$	8.3	10	4.1-9.3
Linolenic	$C_{18:3}$	0.1		0.1-0.2
Arachidic	C_{20}	0.1		0.1-0.3

[a] Calculated from HPLC results (Table 2).

[b] Range of typical analyses found in palm stearine samples from a variety of sources (2).

TABLE 2

Chemical Composition of Palm Stearine by HPLC and GC Analysis

Triglyceride[a]	Content by HPLC mass %	Content by GC mass %[c]	CN	Range mass %[e]
?		1.3	46	0.9-3.0
PPP	13.0	18.5	48	10.2-42.7
PLP	12.6			
POP	33.0	40.2	50	39.4-42.2
SPP	2.4			
PLL	3.7			
PLO	8.0			
SOP	4.4	31.2	52	11.9-37.9
POO	20.3[b]	(14)[d]		
OOO		(6)[d]		
LOO	1.4	8.8	54	2.5-10.3
SOO	1.1			
SOS	0.3			
?		0.4	56	—

[a] Explanation of symbols (Table 1).

[b] Unresolved peak.

[c] Resolution into total carbon number (CN) only.

[d] Estimated from results in columns 2 and 3.

[e] Range of typical analyses found in palm stearine samples from a variety of sources (2).

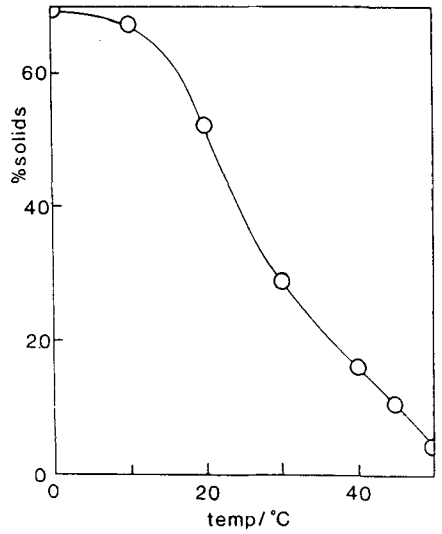

FIG. 1. Effect of temperature on the solid fat content of palm stearine determined by the NMR method. Heat treatment: 60 min at 0°C; 30 min at each (increasing) temperature prior to measurement.

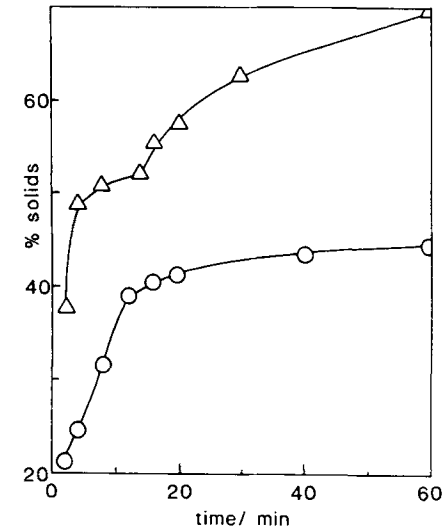

FIG. 2. Solid fat content of palm stearine as a function of the time held at 0°C (triangles), 20°C (circles). Heat pre-treatment 10 min at 60°C (melt).

From the composition of the sample (Table 2) and the melting points of the pure triglycerides (19), the percentage of the sample having melting points in the following ranges can be calculated: greater than 30°C is 53%; between 10° and 30°C is 28% and less than 10°C is 19%. Thus, by inference, it would appear that the first stage of solidification involves a fairly high degree of fractionation so that the solids consist mainly of the high melting triglycerides: PPP, POP, POS, PPS and SOS. Later solidification is apparently much less selective due probably to the occurrence of mixed crystallization and to the solubility of the middle range melting triglycerides (POO, PLP and SOO) in the liquid phase, which will consist mainly of PLO, OOO, PLL and LOO.

Thermal analysis by DSC. The influence of heating rate on the heating scans of palm stearine samples after

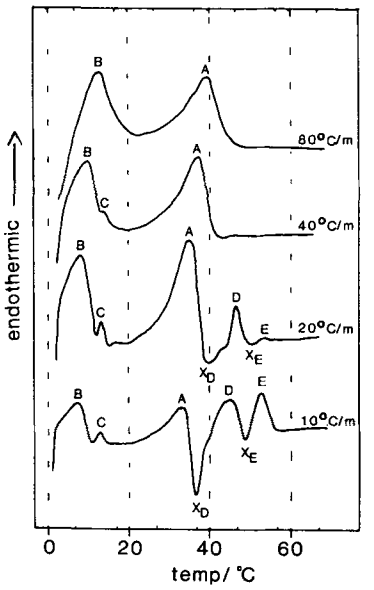

FIG. 3. DSC heating thermograms of palm stearine at heating rates: 80°, 40°, 20°, and 10° min^{-1}. Pre-treatment: cooled from 70° to 0°C at 80° min^{-1}, heating program started after 0.1 min at 0°C. Relative attenuations are 1.6; 1.6; 2.0; 1.0, respectively.

cooling at 80° min^{-1} from the melt and holding for only 6 sec at 0°C is shown in Figure 3. At the highest scan rate of 80° min^{-1}, there is least chance of any structural reorganization occurring during the time of the scan, so that the thermal characteristics observed relate most closely to the morphology of the sample existing at the start of the scan, i.e., at 0°C in this case. Two clear peaks are observed with peak temperatures of 13° and 39.5°C indicating that two melting forms are present in the sample. The ratio of the area of the high melting form to that of the low melting form is roughly 55:45—accurate area measurement was not possible since the leading edge of the first peak coincided with the start of the program. These results suggest that the two melting forms are similar to those observed crystallizing separately at 0°C by the NMR technique.

At lower scan rates, the thermograms contain progressively more shoulders, peaks and valleys indicating that significant structural reorganization is occurring during the DSC scan. Peaks are arbitrarily labelled A, B, C, etc.—in order of appearance and definite exotherms, i.e., positions where the scan crosses below the baseline are labelled X_D, X_E, etc.; the subscript indicates the endotherm to which they appear to relate. As the scanning rate is decreased, the following changes are observed: (i) Endotherm C appears as a minor peak in the lower melting range. (ii) Endotherms D and E and exotherms X_D and X_E appear in the higher melting range. (iii) Endotherm A decreases in size.

These observations suggest that the crystalline form responsible for peak A is undergoing an exothermic rearrangement, under the conditions of the DSC scan, into new crystal forms which melt to give peaks D and E. With less certainty, the form responsible for peak B appears to be transforming to that which melts to give peak C. Even at the lowest scan rate, the maximum time available for structural reorganization in these experiments was

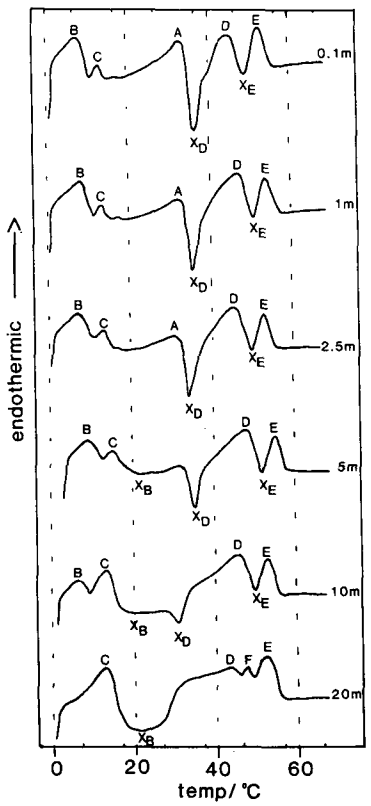

FIG. 4. DSC heating thermograms of palm stearine showing the effect of tempering time at 0°C. Tempering times: 0.1; 1.0; 2.5; 5; 10; 20 min. Pre-treatment: cooled from 70° to 0°C at 80° min^{-1}. Heating rate: 10° min^{-1}.

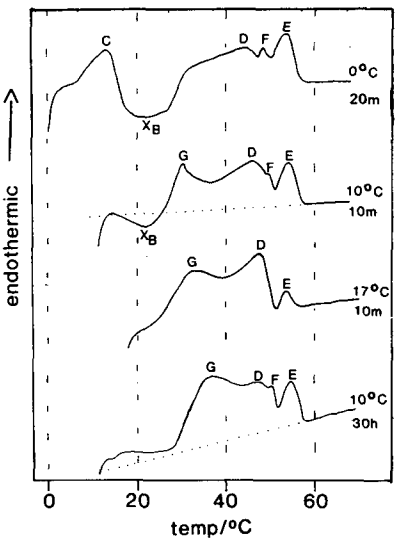

FIG. 5. DSC heating thermograms of palm stearine showing the effect of tempering temperatures: 20 min at 0°C; 10 min at 10°C; 10 min at 17°C; 30 hr at 10°C. Pre-treatment: cooled from 70° to 0°C at 80° min^{-1}, 10 min at 0°C; heated to tempering temperature at 10° min^{-1}; scan rate: 10° min^{-1}.

5 min; less than 1 min in the case of the lower melting form. Further information can be obtained by observing the effect of tempering the sample prior to the DSC scan. The effects of tempering at 0°C for a range of increasing times are shown by the DSC thermograms in Figure 4. The main points are as follows: (i) Endotherm C becomes a major peak as peak B virtually disappears. (ii) A broad exotherm, X_B, appears after longer tempering times, between the low and high melting fractions. (iii) Endotherm A decreases in size and becomes indistinguishable as endotherm D broadens and a new endothermic peak F appears at longer times. (iv) Exotherm X_D decreases and disappears.

These results indicate that in addition to the rearrangement of the high melting form, i.e., that corresponding to peak A being transformed into peaks D and E, the low melting form can also undergo transformations during tempering at 0°C. The disappearance of exotherm X_D and endotherm B suggests that the crystalline form responsible for B is transforming by two pathways: (i) a simple rearrangement to the slightly higher melting form represented by peak C or (ii) to a melt of its mixed crystal structures from which the higher melting fraction can crystallize during the DSC scan into a crystal form giving rise to melting peaks A and/or D and F.

The effects of tempering at the higher temperatures of 10°C and 17°C each for 10 min is shown in Figure 5. The former lies between the peak temperature for peaks B and C and the latter lies just above peak C. The following are the significant observations: (i) Endotherm C has decreased to almost zero while exotherm X_B remains and major endothermic peak G and minor peak F appear. (ii) After the higher tempering temperature of 17°C, endotherm G broadened and endotherms D and F merged into one broad large peak (labelled D in Fig. 5). (iii) Endotherm E decreases after tempering at 17°C.

Observation (i) supports the idea that the crystalline form responsible for peak B undergoes different rearrangements to forms which give rise to peaks G, D and F. The appearance of peak G, which virtually disappeared after long tempering times at 0°C, may be due to the recrystallization of higher melting point triglycerides which would have been trapped in the lower melting (peak B) crystals during tempering at 0°C. As with the long tempering times at 0°C, the crystals melting to give peak D were formed either during tempering or during the early part of the DSC scan; no sharp exotherm, X_D, was observed as in the scans in which peak B was prominent, i.e., after short tempering times at 0°C.

The breadth of peaks G and D following tempering at 17°C may be due to the availability of a greater diversity of triglyceride structures during the crystallization process which gives rise to the crystals melting at G and D. Norton *et al.* (20) have correlated the broadening of melting peaks with an increase in solubility of the crystal structures in the liquid phase.

The decrease in size of peak E is unusual in that high melting crystal forms would only be expected to transform into higher melting forms. The characteristics of the peak are similar to a peak observed by Berger *et al.* (7) when they investigated factors affecting the slip melting point of palm products. They found that a small melting peak at about 50°C, observed by DSC analysis when a sample of palm stearine was tempered at 0°C and at 10°C, did not appear following tempering at 20°C. They explained variations in slip melting point with tempering temperature by the behavior of this peak. It seems likely that some of the crystals responsible for this

peak have dissolved in the liquid phase which is present in greater proportion at the higher tempering temperature.

In one experiment, a sample of the palm stearine was tempered at 10°C for 30 hr. The thermogram run at 10° min^{-1} was very similar to that observed following tempering at 10°C for 10 min (Fig. 5) except that the exothermic transition, X_B, was not present. Thus the increased tempering time had essentially stabilized the sample.

The transitions indicated by the exotherms X_D and X_E occur at temperatures similar to those observed by Persmark *et al.* (1) for the α to β' transition (33°C) and the β' to β transition (44°C) for a high melting solvent fractionated portion of palm oil. They identified the crystal forms by x-ray diffraction. Correlation with this work suggests that peaks A, D and E are due to crystalline material with α, β' and β structure, respectively.

The identification of B, C and F is more difficult than A, D and E as the exothermic transitions are not as sharp as those observed for the higher melting components. The only exotherm visible is a large trough between 15° and 29°C as shown in Figure 4. Persmark *et al.* (1) observed that two fractions could be obtained by crystallization of a solvent fraction of palm oil between 0° and 20°C. The fractions varied in both their CN 52 and CN 54 contents and their $C_{18:1}$ and $C_{18:2}$ content. They attributed the difference between the fractions to the POS (CN 52) and POP (CN 50) contents. A more likely cause, however, might be the difference in PLP and POO contents as they have melting points within the region of the observed transitions (15°-29°C) and are consistent with the variations of the fatty acid distribution reported. They also found that the fraction with the lower CN 52 content and higher $C_{18:2}$ content transformed from sub-α to α structure at −2°C which then transformed to β' structure before melting at 24°C. The higher CN 52 fraction transformed from the sub-α to a mix of α and β' structure at −3°C. At 11°C the fraction transformed into β' structure which transformed into two β structures at 18° and 30°C. This behavior is somewhat similar to that of the low melting component of palm stearine. Structure B which melted between 1° and 10°C is most likely a mix of sub-α and α structures while C is β'. Structure F melting between 38° and 41°C, i.e., too high to be due to the β structures from the lower CN 52 fraction (1), may be due to higher melting triglycerides which have recrystallized in a high melting β' structure following transformation of B to C and then exclusion from the new structure.

When tempered at 10°C, the lower melting components behave more like the higher CN 52 component described by Persmark *et al.* (1). The appearance of G between 27° and 34°C correlates with the behavior of the β component, reported to melt at 30°C. The change in crystallization behavior may be due to some of the triglycerides melting at this temperature and, in effect, changing the composition of the low melting component so that the triglyceride composition of structure C becomes less mixed, thereby allowing transformation into the more stable β structure.

Milk fat has been observed by Timms (21) to behave as a three-component system, each component undergoing transformations independently. He observed that if some low melting component was mixed with the high melting component of milk fat it was possible to transform some of the high melting β' structure into β structure. The high melting component on its own remained in its stable β' form. Thus we can predict that the presence of some low melting components in palm stearine may also enhance β crystal formation in the high melting fraction. It is likely that the low melting components form a mixed crystal structure with some higher melting unsaturated triglycerides leaving the higher melting component with a relatively high level of fully saturated triglycerides. The fully saturated triglycerides could then rearrange to form a β structure.

REFERENCES

1. Persmark, U., K.A. Melin, and P.O. Stahl, *La Rivista Italiana Delle Sostanze Grasse L111*:301 (1976).
2. Rossell, J.B., B. King, and M.J. Downes, *J. Amer. Oil Chem. Soc. 62*:221 (1985).
3. Kawamura, K., *J. Amer. Oil Chem. Soc. 57*:753 (1979).
4. Kawamura, K., *J. Amer. Oil Chem. Soc. 57*:48 (1980).
5. Jacobsberg, B., and Oh Chuan Ho, *J. Amer. Oil Chem. Soc. 53*:609 (1986).
6. Berger, K.G., and W.B. Wright, PRORIM Occasional paper No. 17, Palm Oil Research Institute of Malaysia, Jan. 1986.
7. Berger, K.G., W.L. Siew, and Flingoh C.H. Oh, *J. Amer. Oil Chem. 59*:244 (1982).
8. Defense, E., *J. Amer. Oil Chem. Soc. 62*:376 (1985).
9. Busfield, W.K., and P.N. Proschogo, *J. Amer. Oil Chem. Soc. 67*:150 (1990).
10. Hernqvist, L., Polymorphism of Fats, Ph.D. Thesis, Lund University, Box 740, S-220 07, Lund, Sweden, 1984.
11. Lutton, E.S., *J. Amer. Oil Chem. Soc. 49*:1 (1972).
12. Sato, K., and T. Kuroda, *J. Amer. Oil Chem. Soc. 64*:124 (1987).
13. Melcalfe, L.D., and C.N. Wang, *J. Chrom. Science 19*:530 (1981).
14. Official and Tentative Methods of The American Oil Chemists' Society, 3rd edition, edited by D. Firestone, 1988.
15. Barnicoat, C.R., *Analyst 69*:176 (1984).
16. Deman, J.M., L. Deman, and B. Blackman, *J. Amer. Oil Chem. Soc. 60*:91 (1981).
17. Hamilton, R.J., and J.B. Rossell, *Analyses of Oils and Fats*, Elsevier, London and New York, 1986, p. 377.
18. Timms, R.E., *J. Amer. Oil Chem. Soc. 62*:241 (1985).
19. Timms, R.E., *Palm Oil Product Technology in the Eighties*, T13, Palm Oil Research Institute, Malaysia, 1983.
20. Norton, I.T., C.D. Lee-Tuffnel, S. Ablett, and S.M. Bociek, *J. Amer. Oil Chem. Soc. 62*:756 (1985).
21. Timms, R.E., *Australian J. Dairy Tech.*, 47 (1980).

[Received February 17, 1989; accepted October 12, 1989]
[J5665]